Published in final edited form as:

Nat Chem Biol. 2018 January ; 14(1): 8–14. doi:10.1038/nchembio.2512.

Purinyl-cobamide is a native prosthetic group of reductive dehalogenases

Jun Yan[1,2,3,4,5,*], **Meng Bi**[1], **Allen K. Bourdon**[6], **Abigail T. Farmer**[6], **Po-Hsiang Wang**[7], **Olivia Molenda**[7], **Andrew Quaile**[7], **Nannan Jiang**[3,4,5,8], **Yi Yang**[3,9], **Yongchao Yin**[1], **Burcu Şimşir**[3,9], **Shawn R. Campagna**[6], **Elizabeth A. Edwards**[7], and **Frank E. Löffler**[1,3,4,5,8,9,10,*]

[1]Department of Microbiology, University of Tennessee, Knoxville, Tennessee 37996, USA

[2]Key Laboratory of Pollution Ecology and Environmental Engineering, Institute of Applied Ecology, Chinese Academy of Sciences, Shenyang, Liaoning 110016, P.R. China

[3]Center for Environmental Biotechnology, University of Tennessee, Knoxville, Tennessee 37996, USA

[4]Biosciences Division, Oak Ridge National Laboratory, Oak Ridge, Tennessee 37831, USA

[5]Joint Institute for Biological Sciences (JIBS), Oak Ridge National Laboratory, Oak Ridge, Tennessee 37831, USA

[6]Department of Chemistry, University of Tennessee, Knoxville, Tennessee 37996, USA

[7]Department of Chemical Engineering and Applied Chemistry, University of Toronto, Toronto, Ontario, M5S 3E5, Canada

[8]Bredesen Center for Interdisciplinary Research and Graduate Education, University of Tennessee, Knoxville, Tennessee 37996, USA

[9]Department of Civil and Environmental Engineering, University of Tennessee, Knoxville, Tennessee 37996, USA

[10]Department of Biosystems Engineering & Soil Science, University of Tennessee, Knoxville, Tennessee 37996, USA

Abstract

*Corresponding authors: Frank E. Löffler: frank.loeffler@utk.edu Jun Yan: junyan@iae.ac.cn.
Correspondence and requests for materials should be addressed to J.Y. and F.E.L.

Author contributions: F.E.L., J.Y. and S.R.C. conceptualized the research and designed experiments. J.Y., M.B., B.S., Y. Yang, and Y. Yin performed cultivation work, corrinoid extraction and purification, and phylogenetic analyses. A.K.B and A.T.F. performed LC-MS and structural analyses. P.W., O.M. and A.Q. performed BN-PAGE, enzyme assays and proteomic analysis. N.J. generated *cobT* expression clones. All authors contributed to data analysis and interpretation, and J.Y., S.R.C., E.A.E. and F.E.L. wrote the manuscript.

Competing financial interests

The authors declare no competing financial interests.

Additional Information.

Any supplementary information, chemical compound information and source data are available in the online version of the paper.

Cobamides such as vitamin B_{12} are structurally conserved, cobalt-containing tetrapyrrole biomolecules with essential biochemical functions in all domains of life. In organohalide respiration, a vital biological process for the global cycling of natural and anthropogenic organohalogens, cobamides are the requisite prosthetic groups for carbon–halogen bond-cleaving reductive dehalogenases. This study reports the biosynthesis of a new cobamide with unsubstituted purine as the lower base, and assigns unsubstituted purine a biological function by demonstrating that Coα-purinyl-cobamide (purinyl-Cba) is the native prosthetic group in catalytically active tetrachloroethene reductive dehalogenases of *Desulfitobacterium hafniense*. Cobamides featuring different lower bases are not functionally equivalent, and purinyl-Cba elicits different physiological responses in corrinoid-auxotrophic, organohalide-respiring bacteria. Given that cobamide-dependent enzymes catalyze key steps in essential metabolic pathways, the discovery of a novel cobamide structure and the realization that lower bases can effectively modulate enzyme activities generate opportunities to manipulate functionalities of microbiomes.

Introduction

Corrinoids are the most complicated organometallic cofactors biology uses to catalyze essential biochemical reactions including methyl group transfer, carbon skeleton rearrangement and reductive dehalogenation[1]. Complete corrinoids (i.e., cobamides) consist of an upper Coβ ligand, a central cobalt-containing corrin ring, and a lower Coα base as part of the nucleotide loop that is connected to the corrin ring[2]. For example, vitamin B_{12} (cyanocobalamin) carries the artificial cyano group as an upper Coβ ligand and 5,6-dimethylbenzimidazole (DMB) as the lower base (Fig. 1). Variations in cobamide (Cba) structure exist in the upper ligand, the lower base, and, in one documented case, the side chain in the nucleotide loop[3]. Physiologically functional cobamides use a methyl group or a 5′-deoxyadenosyl moiety as the upper ligand, and one of 16 known lower bases connected to the nucleotide loop[2] (Fig. 1). Reductive dehalogenation reactions can be mediated abiotically by vitamin B_{12} and its analogues in the presence of a strong reductant capable of generating the cobalt(I) supernucleophile[4], or can be catalyzed by corrinoid-dependent reductive dehalogenases (RDases)[5]. In either case, the cobalt(I) supernucleophile is critical for the initiation of carbon–halogen bond cleavage[6].

Recently resolved RDase crystal structures of NpRdhA (PDB ID 4RAS) from *Nitratireductor pacificus* and PceA (PDB ID 4UR0) from *Sulfurospirillum multivorans* demonstrate that their prosthetic groups coenzyme B_{12} and norpseudo-B_{12}, respectively, are in the base-off configurations, indicating that their respective lower bases DMB and adenine, are uncoordinated and distant from the redox-active cobalt atom[7,8]. Therefore, the lower base is not assigned a direct role in catalysis or electron transfer to restore the reactive cobalt(I) state. Contrary to expectations, lower base structure does impact reductive dechlorination rates and growth of obligate organohalide-respiring, corrinoid-auxotrophic *Dehalococcoides mccartyi* (*Dhc*) strains[9,10]. Maximum reductive dechlorination activity and *Dhc* growth require the addition of cobamides carrying DMB or 5-methylbenzimidazole (5-MeBza) as the lower base, and cobamides with other lower base structures compromise growth (i.e., 5-methoxybenzimidazole, 5-OMeBza; benzimidazole, Bza), or cause complete loss of reductive dechlorination activity (i.e, 5-hydroxybenzimidazole, 5-OHBza;

adenine)[10,11]. The lower base structure also affects substrate utilization in the homoacetogen *Sporomusa ovata*, which uses phenolic cobamide-dependent methyltransferases for energy conservation and carbon assimilation using the Wood–Ljungdahl pathway[12]. The addition of 5-MeBza or DMB to the medium results in the formation of non-native 5-methylbenzimidazolyl-cobamide (5-MeBza-Cba) or cobalamin, respectively, severely inhibiting growth with methanol or 3,4-dimethoxybenzoate as substrates[12]. These findings indicate that the lower bases can affect enzyme activity with substantial consequences to the host organisms, but mechanistic understanding is lacking. To date, 16 naturally occurring lower bases have been identified, mostly from anaerobic bacteria, with the most recent structure, phenol in phenolyl-cobamide of *Sporomusa ovata* (Fig. 1), discovered in 1989[13].

Members of the genus *Desulfitobacterium* (*Dsf*) are strictly anaerobic, metabolically versatile, Gram-positive bacteria common in subsurface environments, where they contribute to the reductive dehalogenation of organohalogens, including groundwater contaminants such as chlorinated solvents[14,15]. The tetrachloroethene (PCE) RDases have a strict requirement for cobamide as a prosthetic group and generate predominantly *cis*-1,2-dichloroethene (*c*DCE) and inorganic chloride as products[16]. The characterized PCE-dehalogenating *Dsf* pure cultures grow in defined medium without exogenous corrinoids, indicating that these *Dsf* strains are capable of *de novo* corrinoid biosynthesis[17]. Genome sequence analysis corroborates that *Dsf* strains possess the complete set of genes required for cobinamide biosynthesis and lower base activation and attachment, but the identity of the lower base of native *Dsf* cobamide(s) remains elusive[18].

Here we report the discovery and characterization of purinyl-cobamide (purinyl-Cba, **1**) as the native cobamide produced in axenic PCE-dechlorinating *Dsf* cultures, and demonstrated its distinct functionality in different corrinoid-auxotrophic organohalide-respiring bacteria. Direct detection of purinyl-Cba was achieved in catalytically active PCE RDase following electrophoretic separation, illustrating an innovative approach for rapid characterization of corrinoid prosthetic groups. The results obtained expand the diversity of naturally occurring cobamide structures, and assign a biological function to unsubstituted purine.

RESULTS

Discovery and structure of a novel cobamide

High-performance liquid chromatography (HPLC) analysis of the cyanated form (e.g., a cyano group as the upper β-ligand) of corrinoid extracts from PCE-grown *Dsf* pure cultures (i.e., *Dsf* strains Y51, JH1, Viet1 and PCE1) revealed the presence of three candidate corrinoids with retention times of 11.79 min (**1**), 15.74 min (**2**) and 15.95 min (**3**) (Fig. 2a and Supplementary Results, Supplementary Fig. 1a). Integrated peak areas at 361 nm of the total fractions eluting between 10 and 18 min (i.e., the range of retention times for seven Cba standards, **4**–**10;** Fig. 2a) determined that the predominant corrinoid produced in the *Dsf* cultures was associated with the 11.79 min fraction. This retention time was different from cobinamide (Cbi) (which eluted at 8.77 min as monocyano-Cbi and 15.63 min as dicyano-Cbi[19], Supplementary Fig. 1b) and any of the cobamide standards, indicating that the *Dsf* strains produced a distinct corrinoid. The UV-Vis spectrum of the predominant *Dsf hafniense* strain Y51 corrinoid (**1**) substantially overlapped with that of vitamin B_{12} (**10**),

including the 361 nm absorption maximum, but was distinct from the Cbi spectrum with a 355 nm absorption maximum (Fig. 2b). Two minor fractions that eluted after the predominant *Dsf* corrinoid showed absorption spectra and retention times (15.74 and 15.95 min) similar to Cbi, suggesting that these minor fractions may represent Cbi precursors (Supplementary Fig. 2).

Mass spectra of the *Dsf hafniense* strain Y51 corrinoid and of vitamin B_{12} standard obtained using liquid chromatography-mass spectrometry (LC-MS) displayed strong base peaks with *m/z* values of 1,329.54 and 1,355.58, respectively, which corresponded to intact corrinoid ions $[M+H]^+$ (Supplementary Fig. 3a,b). The base peaks with *m/z* values of 1,351.52 and 1,377.56 represented the $[M+Na]^+$ ion form of the strain Y51 corrinoid and vitamin B_{12}, respectively. The mass spectra of the predominant corrinoids from *Dsf* strains JH1, Viet1 and PCE1 matched that of *Dsf hafniense* strain Y51, showing base peaks with *m/z* values of 1,329.54 and 1,351.52 corresponding to their $[M+H]^+$ and $[M+Na]^+$ ion forms, respectively (Supplementary Fig. 3c,d,e). Since the molecular mass of the alpha-ribazole-5′-phosphate (α-RP) moiety in natural cobamides ranges from 306.2 (with phenol as the lower base) to 425.31 Da (with 2-methylsulfonyladenine as the lower base), a mass difference of 312.42 Da between the measured molecular mass of the *Dsf* corrinoid and the calculated molecular mass of Cbi (1016.12 Da in the monocyano form) indicated that the predominant *Dsf* corrinoid was a cobamide carrying an α-RP moiety with a yet-unidentified lower base. Comparisons with the calculated masses of naturally occurring cobamides in their cyanated form suggested that the organohalide-respiring *Dsf* strains produce a unique cobamide distinct from any currently known natural cobamide. Based on mass information, a possible molecular formula for the *Dsf* cobamide was deduced as $C_{59}H_{82}CoN_{16}O_{14}P$.

In the nor-type corrinoid produced by *Sulfurospirillum multivorans*, C_{176} of the side chain is demethylated[3] (Fig. 1). To test if demethylation or any other modification exists in the cobinamide structure of this novel *Dsf* cobamide, we grew *Dsf hafniense* strain Y51 cultures with PCE as electron acceptor in the presence of 25 μM DMB. The addition of DMB was shown to trigger the synthesis of a non-native cobamide[12,20]. This guided cobamide biosynthesis approach with strain Y51 resulted in the formation of cobalamin, as determined by HPLC retention time, UV-Vis spectrum (Fig. 2c,d), and mass spectral features with two strong peaks with *m/z* values of 1,355.58 ($[M+H]^+$) and 1,377.56 ($[M+Na]^+$) (Supplementary Fig. 3f). Similarly, we detected exclusively Bza-Cba (**5**) in strain Y51 cultures that received Bza (Supplementary Fig. 4). Guided cobamide biosynthesis does not change the assembly of the cobinic acid skeleton as prior studies have suggested[20,21]. Thus, similar PCE-to-*c*DCE dechlorination performance in strain Y51 cultures producing the *Dsf* native cobamide, cobalamin, or Bza-Cba indicated that the different prosthetic groups supported functionality of the *Dsf* PceA RDase. Collectively, these findings confirmed that the new cobamide natively synthesized in *Dsf* strains did not possess any unusual modifications. Based on this information, we estimated the molecular mass of the lower base compound in the *Dsf* cobamide to be 120.15 (1,329.54 ($[M+H]^+$ of cyanated *Dsf* cobamide) – [1,355.58 ($[M+H]^+$ of cyanocobalamin) – 146.19 (DMB)]), suggestive of unsubstituted purine.

Confirmation of the novel lower base structure

The cobinic acid skeleton in the cyanated form carries a constant number of 12 nitrogen atoms. Depending on the lower base, naturally occurring cobamides possess 12 to 17 nitrogen atoms. Thus, the number of nitrogen atoms distinguishes a cobamide with an unsubstituted purine as the lower base (12+4 = 16 nitrogen atoms) from cobamides that carry nucleobases (e.g., adenine or guanine, 12+5 = 17 nitrogen atoms), Bza (12+2 = 14 nitrogen atoms) or phenol derivatives (12+0 = 12 nitrogen atoms). Based on these structural characteristics, we conducted ^{15}N isotope-labeling experiments with *Dsf hafniense* strain Y51 to determine the number of nitrogen atoms in the unknown lower base structure. The *m/z* values for the base peaks of the $[M+H]^+$ and $[M+Na]^+$ ion forms of the ^{15}N-labeled cobamide shifted from 1,329.54 to 1,344.48 and 1,351.52 to 1,366.46, respectively, corresponding to a 14.94 Da mass increase (Fig. 2e). Based on this mass shift, we calculated that the total number of nitrogen atoms in the native *Dsf* cobamide is 16 (15 plus one unlabeled nitrogen in the upper CN ligand), indicating that the lower base contains 4 nitrogen atoms (i.e., 16–12). Hypoxanthine, a purine derivative with 4 N atoms, is the lower base of a native cobamide in *Desulfovibrio vulgaris*[22]; however, hypoxanthine-Cba in its cyanated form has a calculated molecular mass of 1,345.29, which is different from the measured $[M+H]^+$ *m/z* value of 1,329.54 for the *Dsf* cobamide. Collectively, ^{15}N isotope labeling followed by mass spectrometry analysis provided additional evidence that unsubstituted purine served as the lower base in the native *Dsf* cobamide.

To confirm unsubstituted purine as a new naturally occurring lower base, we conducted 1D and 2D nuclear magnetic resonance spectroscopy (NMR) experiments with the native *Dsf* cobamide. The superimposed ^1H NMR spectra (Fig. 2f) of authentic vitamin B_{12} (**10**) and the purified native *Dsf* cobamide (**1**) revealed that the only notable changes (i.e., chemical shifts) occurred in the aromatic region (9.0–6.0 p.p.m.), which was primarily associated with the DMB portion of vitamin B_{12}. Homonuclear correlation spectroscopy (COSY) experiments with the *Dsf* cobamide and vitamin B_{12} (Supplementary Fig. 5) revealed spin-spin coupling between neighboring protons, but the spectra differed in the aromatic region. The lower base aromatic protons in the *Dsf* cobamide lacked correlation with other protons in the molecule, suggesting the aromatic moiety does not have any adjacent protons. Hydrogen atoms A, B, and C in Figure 2f directly correlate with the three hydrogen atoms of purine. In comparison, the vitamin B_{12} COSY spectrum demonstrated direct correlations between the benzyl protons (7.3 and 6.5 p.p.m.) and the adjacent methyl group (2.2 p.p.m.) of the DMB moiety. These experiments supported the assignment of unsubstituted purine as the lower base of native *Dsf* cobamide. Purine-containing compounds can exist as four regioisomers through covalent bonding at each of the N-heteroatoms, but the limited amount of purinyl-Cba extractable from *Dsf* cultures did not allow for stereoisomer confirmation by ^{13}C and/or ^{15}N NMR spectroscopic analyses. Prior research has shown that the 9-H and 7-H purine tautomers of purine are favored over 3-H and 1-H purine due to increased aromaticity (tautomer stability: 9-H>7-H>3-H>1-H)[23]. Based on these observations and precedence for purines to form bonds with an imidazole nitrogen[24], the N-glycosidic bond was inferred to be analogous to that observed in other biomolecules. This combined suite of analytical techniques offers a practical approach for lower base characterization and can aid in the discovery of new corrinoids.

Purinyl-Cba is the prosthetic group of *Dsf* PceA RDases

Mature *Dsf* PceA RDases are in the 50–60 kDa mass range[14,16], but maximum reductive dechlorination activity is generally associated with bands excised from blue native polyacrylamide gel electrophoresis (BN-PAGE) gels in the 242–480 kDa region, presumably due to complexation with other proteins[25]. Following the non-denaturing separation of *Dsf hafniense* strain JH1 crude extracts (Supplementary Fig. 6), the highest dechlorination activity was associated with gel slice #4, whereas the other five gel slices exhibited no detectable or negligible (<8%) *c*DCE production from TCE (Fig. 3a). Subsequent in-gel extraction recovered corrinoid from gel slice #4 but not from slices #3 and 5, and ultra-performance liquid chromatography-high resolution mass spectrometry (UPLC-HRMS) revealed that the corrinoid associated with gel slice # 4 and the purinyl-Cba standard (Fig. 3b,c) had matching retention times and *m/z* values. The proteomic analysis of gel slices #3, 4, and 5 demonstrated that the *Dsf* PceA RDase (WP_011460641.1) was enriched in gel slice # 4 along with carbon monoxide dehydrogenase (CODH) and FAD-dependent fumarate reductase, which are both corrinoid-independent enzymes (Supplementary Table 1)[26,27]. CODH may occur in complexes with corrinoid-dependent, Wood–Ljungdahl pathway enzymes (e.g., 5-methyltetrahydrofolate-homocysteine methyltransferase), but no such proteins were detected in gel slice #4. Purinyl-Cba was the only corrinoid detected in this gel slice, confirming that the *Dsf* PceA RDase uses purinyl-Cba as the native prosthetic group.

Dsf CobT substrate specificity and phylogenetic analysis

The nicotinate-nucleotide-dimethylbenzimidazole phosphoribosyltransferase (CobT) activates lower bases to their respective α-RP forms (Fig. 4a), and the CobT substrate specificity determines the type of cobamide produced[19]. CobT sequences encoded in sequenced *Dsf* genomes are highly conserved (81.3–100% amino acid identity) except for *Dsf metallireducens* strain DSM 15288, whose CobT shares no more than 58.5% amino acid identity with other available *Dsf* CobT sequences. A broader phylogenetic analysis clustered bacterial CobT sequences into distinct clades, which reflected the substrate specificities (i.e., lower base type that is activated) of characterized CobT, and provided clues about the native cobamides produced by the respective host organisms (Fig. 4b and Supplementary Table 2). This analysis further revealed that the *Dsf* CobT clade was distinct (<52% amino acid identity) from any other CobT implicated in phenol/*p*-cresol, adenine, guanine/hypoxanthine or Bza-type lower base activation. The most closely related sequences to the *Dsf* CobT clade (except for *Dsf metallireducens* CobT) were found in *Dehalobacter* (*Dhb*) and *Desulfosporosinus* (i.e., *Desulfosporosinus youngiae* strain DSM 17734, CM001441.1; *Desulfosporosinus meridiei* strain DSM 13257, CP003629.1; *Desulfosporosinus orientis* strain DSM 765, CP003108.1) genomes, with 57.8–59.3% and 56.6–61.7% amino acid identity, respectively (Fig. 4b); however, the native corrinoids produced in either *Dhb* or *Desulfosporosinus* spp. strains have not yet been identified. The high CobT sequence identities among these members of the Peptococcaceae suggested that purine activation to the α-RP derivative is a shared feature of this family (Fig. 4b).

Cultivation work indicates that *Dhc* CobT utilizes a variety of benzimidazole-type lower bases with a preference for DMB[10,11]. *In vitro* enzyme assays with purified *Dsf* CobT and *Dhc* CobT (Supplementary Fig. 7a) with nicotinic acid mononucleotide (NaMN) and purine

or DMB as substrates verified that *Dsf* CobT and *Dhc* CobT both activated DMB to the α-RP form of DMB (α-RP [DMB]) (Fig. 4c), consistent with the observation that exogenous DMB guided *Dsf* to produce cobalamin as a non-native prosthetic group of the PceA RDase. The *Dsf* and *Dhc* CobT enzymes activated DMB (250 μM), and 166.9 ± 2.70 and 159.4 ± 1.13 μM α-RP [DMB], respectively, were produced following a 30-min incubation period (Fig. 4d). In *Dsf* CobT assays with purine (250 μM) replacing DMB, the conversion yield to α-RP [purine] exceeded 99% after a 30-min incubation period (Fig. 4c,d). In assays with *Dhc* CobT, purine was not consumed, no α-RP [Purine] was produced, and only small amounts of nicotinate were observed, indicating that *Dhc* CobT was unable to activate unsubstituted purine (Fig. 4c,d). No α-RP formation occurred in controls lacking NaMN, a lower base, or CobT, corroborating that *Dsf* CobT catalyzed the activation of unsubstituted purine to α-RP [purine] (Supplementary Fig. 7b). MS analysis performed on fractions containing CobT enzyme assay products showed strong adducts with *m/z* ($[M+H]^+$) values of 359.10 and 333.06, respectively, matching the calculated molecular mass of α-RP [DMB] and α-RP [purine] (Fig. 4e). These findings demonstrated an unprecedented *Dsf* CobT specificity for unsubstituted purine, consistent with the discovery of purinyl-Cba as the native prosthetic group of *Dsf* PceA.

Effects of purinyl-Cba on dechlorinating activity

To test if purinyl-Cba supports corrinoid-dependent reductive dechlorination in corrinoid-auxotrophic organohalide-respiring bacteria, we grew axenic *Dhb restrictus* strain PER-K23 and *Dhc* cultures with purinyl-Cba. Strain PER-K23 harbors a PceA RDase with 98.7% amino acid identity to the PceA of *Dsf hafniense* strain Y51. Strain PER-K23 cultures that received 36.9 nM of vitamin B_{12} (positive control) or purinyl-Cba completely dechlorinated the initial amount of 64.4 ± 2.3 μmoles of PCE to *c*DCE within 6 days at statistically indifferent rates of 427 ± 25 and 471 ± 39 μM Cl^- released per day, respectively (Fig. 5a). Much lower dechlorination rates of 23.7 ± 9.3 μM Cl^- released per day, resulting in the formation of small amounts of trichloroethene (TCE) (8.2 ± 2.5 μmoles) and *c*DCE (5.4 ± 2.5 μmoles), occurred in control incubations without exogenous corrinoid (Fig. 5a). Strain PER-K23 cell numbers increased about 50-fold in purinyl-Cba- and vitamin B_{12}-amended cultures, whereas growth was negligible in control cultures without corrinoid addition (Supplementary Table 3). Biomass from purinyl-Cba- and vitamin B_{12}-fed *Dhb* cultures contained exclusively purinyl-Cba and vitamin B_{12}, respectively, indicating that cobamide or lower base modifications did not occur (Fig. 5b). These findings demonstrated that both *Dhb restrictus* strain PER-K23 and *Dsf hafniense* strain Y51 PceA RDases were fully functional with either purinyl-Cba or cobalamin as the prosthetic group.

Corrinoid-auxotrophic *Dhc* pure cultures demonstrated a different response to purinyl-Cba. *Dhc* strains BAV1 and GT express the BvcA and VcrA RDase, respectively, which share less than 20% amino acid identity with the *Dsf* and *Dhb* PceA RDases. Complete reductive dechlorination of *c*DCE to ethene occurred in vitamin B_{12}-amended *Dhc* strain BAV1 and strain GT cultures at rates of 201 ± 11 and 197 ± 10 μM Cl^- released per day, respectively (Fig. 5c and Supplementary Fig. 8). Strain BAV1 and strain GT cultures with purinyl-Cba as the sole corrinoid amendment exhibited much slower *c*DCE dechlorination rates of 17.6 ± 1.2 and 11.7 ± 0.7 μM Cl^- released per day, respectively (Fig. 5c and Supplementary Fig.

8). After a 32-day incubation period, the cultures dechlorinated about half of the initially supplied *c*DCE (83 μmoles) but produced no ethene. In control cultures without exogenous corrinoid, strain BAV1 and strain GT dechlorinated no more than 22% and 7.3%, respectively, of the initial *c*DCE to vinyl chloride (presumably enabled by corrinoid carryover with the inoculum), and formed no ethene (Fig. 5c and Supplementary Fig. 8). Consistent with the observed reductive dechlorination activity, 16S rRNA gene enumeration indicated robust *Dhc* growth in cultures amended with vitamin B_{12} but not in cultures that received purinyl-Cba (Supplementary Table 3). In contrast to the PceA RDases, the *Dhc* RDases BvcA and VcrA had a pronounced preference for DMB over unsubstituted purine as the lower base, emphasizing that the lower base can modulate the activity of corrinoid-dependent RDases[10].

DISCUSSION

The purine structure is the most widely distributed nitrogen-containing heterocycle in nature, and purine derivatives fulfill many essential functions in biological systems[28]. Obvious examples of purine derivatives include adenine and guanine, which are essential building blocks of nucleic acids, and ubiquitous molecules like adenosine 5′ triphosphate (ATP), nicotinamide adenine dinucleotide (NAD^+, NADH), and flavin adenine dinucleotide (FAD, $FADH_2$)[28]. Remarkably, compounds containing an unsubstituted purine moiety are rare and a specific biological function has never been assigned to purine itself. To date, nebularine (purine nucleoside) is the only known biological compound that contains unsubstituted purine. Nebularine was first isolated from the fungus *Clitocybe nebularis*[29] and is also produced by *Streptomyces yokosukanensis*[30] and a *Microbispora* isolate[31]. Nebularine is a potent antibiotic against various *Mycobacterium* species, exhibits cytotoxic effects in cell cultures and plants[32,33], and is toxic to the schistosomiasis (bilharzia) parasite[34]; however, its biological functions for the hosts are unclear. In *S. yokosukanensis*, nebularine biosynthesis involves a single enzyme catalyzing the reductive deamination of adenosine[35]. Apparently, at least some members of the domains Bacteria and Eukaryota synthesize unsubstituted purine indicating that purine is not a xenobiotic, a finding with potential human health implications. Purinergic membrane receptors, which include the adenosine-responsive P1 purinoceptors, are found in almost all mammalian tissues, where they fulfill crucial functions that can affect disease progression[36–38]. Although the occurrence of unsubstituted purine in mammals is not established, the simple enzymatic conversion of adenosine to nebularine has been demonstrated[35], and enzymatic hydrolysis of the N-glycosidic bond catalyzed by common nucleoside hydrolases (i.e., purine nucleosidases) releases the corresponding free bases[24]. Thus the formation of unsubstituted purine (or purine nucleoside) could affect the regulation of cellular functions (purinergic signaling), potentially enabling novel disease therapies. Purinyl-Cba synthesis using *Dsf* CobT will facilitate detailed investigations of its therapeutic potentials.

Corrinoid-dependent enzyme systems fulfill essential metabolic functions for organisms in all branches of life, but only some members of the Bacteria and Archaea have the machinery for *de novo* corrinoid biosynthesis[1,2,39–42]. The discovery of a new member of the corrinoid family of molecules, purinyl-Cba in organohalide-respiring members of the Peptococcaceae, expands the number of naturally occurring, functional lower base structures, and assigns a

function to unsubstituted purine in biological systems. From this study and recent reports, the concept emerges that lower base structures are modulators of corrinoid-dependent enzyme function[10,12,20,21]. This concept applies to the *Dhc* RDases but possibly expands to many other corrinoid-dependent enzyme systems, emphasizing that enzyme-specific corrinoid cofactor requirements must be understood to predict, and possibly manipulate, catalytic activity (e.g., *Dhc* reductive dechlorination rates and extents)[43]. The exact role(s) of the lower base for RDase function is not resolved, but recent findings reveal a base-off configuration during catalysis[7,8]. If not directly involved in catalysis, the lower base structures may affect holoenzyme maturation, or, in the case of periplasmic enzymes such as respiratory RDases, export through the cytoplasmic membrane. Cobamides fulfill essential metabolic functions for the majority of organisms, including mammals, and the principle of lower base-controlled activity of key corrinoid-dependent enzyme systems may provide new avenues to manipulate environmental (e.g., bioremediation) and biotechnological (e.g., anaerobic digestion, biogas production) processes, and to expand treatment options to affect progression of relevant human diseases.

ONLINE METHODS

Chemicals

Vitamin B_{12} (≥98%), dicyanocobinamide (Cbi, ≥93%), 5,6-dimethylbenzimidazole (DMB) (99%), 5-methylbenzimidazole (5-MeBza) (98%), 5-methoxybenzimidazole (5-OMeBza) (97%), benzimidazole (Bza) (98%), purine (98%) were purchased from Sigma-Aldrich. $^{15}NH_4Cl$ (99%) was obtained from Cambridge Isotope Laboratories. Yeast extract and peptone were purchased from Becton, Dickinson and Company. Bza-Cba, 5-MeBza-Cba and 5-OMeBza-Cba were prepared via guided cobamide biosynthesis [10]. Factor III (5-OHBza-Cba), norpseudo vitamin B_{12} and phenolic cobamides (i.e., Phenol-Cba and *p*-Cresol-Cba) were extracted and purified from *Methanosarcina barkeri* strain Fusaro (DSM 804), *Sulfurospirillum multivorans* (DSM 12446) and *Sporomusa* sp. strain KB-1 (16S rRNA gene GenBank accession no. AY780559.1) cells, respectively. Concentrations of purified cobamides were determined at 361 nm with a Lambda 35 UV-Vis spectrometer (PerkinElmer) using a molar extinction coefficient of 28,060 $mole^{-1}$ cm^{-1} [12]. Ethene (≥99.9%) and vinyl chloride (≥99.5%) were purchased from Sigma-Aldrich. All other chemicals used were reagent grade or higher.

Cultures

Pure cultures were grown in 160-mL glass serum bottles containing 100 mL of bicarbonate (30 mM) or phosphate (50 mM) buffered, defined mineral salts medium, the Wolin vitamin mix excluding vitamin B_{12}, and a N_2/CO_2 (80/20, v/v) headspace. *Dsf hafniense* strains Y51 and JH1 and *Dsf* sp. strains Viet1 and PCE1 cultures were supplemented with pyruvate (10 mM) as fermentable substrate, and PCE (68 μmoles per bottle, 0.48 mM aqueous concentration) as electron acceptor [44]. *Dhc* strain BAV1 and strain GT cultures were amended with 5 mM acetate as carbon source, 10 mL hydrogen as electron donor, neat *c*DCE (79 μmoles per bottle, 0.60 mM aqueous concentration) as electron acceptor, and a cobamide (e.g., vitamin B_{12}) as described [10]. *Geobacter sulfurreducens* strain PCA cultures received 5 mM acetate as electron donor and 10 mM fumarate as electron acceptor as

described [45]. *Sulfurospirillum multivorans* strain DSM 12446 cultures were grown with pyruvate (10 mM) and neat PCE (0.48 mM) as electron acceptor as described [21]. *Dhb restrictus* strain PER-K23 cultures were amended with 5 mM acetate as carbon source, 10 mL hydrogen as electron donor, neat PCE (0.48 mM) as electron acceptor, and peptone (0.5 g/L) as source of required amino acids [46]. *Sporomusa* sp. strain KB-1 cultures were amended with betaine (50 mM) as the sole substrate [20]. *Methanosarcina barkeri* strain Fusaro was grown with 123 mM methanol as the sole substrate [20]. All vessels were incubated without agitation in the dark at 30 °C. For ^{15}N isotope experiments, $^{15}NH_4Cl$ (0.3 g/L) replaced unlabeled NH_4Cl as the nitrogen source. L-cysteine, a reductant added to the medium, is a potential nitrogen source and was omitted in the labeling experiments. $^{15}NH_4Cl$-grown cultures were transferred (1% inoculum, v/v) twice in 160-mL serum bottles containing 100 mL of medium before scaling up to a 2.2-liter vessel containing 1.8 liter of medium in order to extract sufficient ^{15}N-labeled corrinoid for LC-MS analysis. Initial experiments with *Geobacter sulfurreducens* strain PCA, a bacterium that natively produces 5-OHBza-Cba (14 N atoms in the cyano form) [47], demonstrated the utility of the ^{15}N isotope labeling approach to determine the number of N atoms in the lower base structure. We found that the mass spectra of ^{15}N-labeled versus unlabeled 5-OHBza-Cba produced in *Geobacter sulfurreducens* cultures amended with $^{15}NH_4Cl$ versus NH_4Cl returned a mass shift of 12.96 Da, close to the expected value of 13 total N atoms (14 minus one unlabeled N in the upper CN ligand, which was added during the KCN extraction process) (Supplementary Fig. 9.

Corrinoid extraction

Cells were harvested from 0.3–1.8 liter culture suspensions by centrifugation at 15,000 × g for 15 min at 4 °C, or by filtration onto 47 mm diameter 0.22 μm pore size polyethersulfone membrane filters (Pall Life Sciences). The intracellular corrinoids were extracted from the biomass following an established KCN extraction protocol and purified using a C18 Sep-Pak cartridge (Waters Corp) [10]. To extract corrinoids from proteins separated by BN-PAGE, gel slices were excised and transferred to individual 2-mL plastic tubes containing 1 mL of 90% (v/v) methanol containing 50 mM acetic acid and 10 mM KCN (final pH 5.5) for corrinoid extraction. The closed tubes were incubated at 60 °C for 2 hours to solubilize corrinoids, before the solution was transferred to new 2-mL plastic tubes and vacuum dried using a rotary evaporator at 45 °C for 2 hours. The dry residues were suspended in 75 μL ice-cold ammonium acetate (20 mM, pH 6.0) and centrifugation at 13,000 × g for 5 min at 4 °C removed insoluble Coomassie Blue dye and gel residuals.

Corrinoid analysis

Intracellular corrrinoids were analyzed by HPLC, UV-Vis spectroscopy, and UPLC-HRMS. HPLC analysis was performed with an Eclipse XDB-C18 column (Agilent Technologies, 5 μm pore size, 4.6 mm inner diameter × 250 mm length) operated at a flow rate of 1 mL per min at 30 °C using 0.1% (v/v) formic acid (≥88%, w/v, Thermo Fisher, Waltham, MA, USA) in water as eluent A and 0.1% (v/v) formic acid in methanol as eluent B. The initial mobile phase composition was 82% eluent A and 18% eluent B, before the fraction of eluent B increased linearly to 25% over a 12-min and further to 75% over an additional 3-min time period, held at 75% B for 5 min before restoring initial column conditions. UV-Vis spectra

between 250 to 600 nm were collected using a diode array detector. The upper ligand, cobalt oxidation state, and lower base coordination influence the corrinoid absorbance spectrum in the UV region [42]. All corrinoid samples and standards in this study carried the cobalt atom in the fully oxidized +3 state and a cyano group as the upper ligand. Cbi lacks the entire alpha-ribazole-5′-phosphate (α-RP) moiety and exhibited an UV-Vis spectrum with an absorption peak at 355 nm, distinct from the 361 nm absorption peak of vitamin B_{12} (Fig. 2b). The corrinoids extracted from BN-PAGE gels were analyzed using an UltiMate 3000 UPLC system in tandem with a high-resolution Exactive Plus Orbitrap mass spectrometer (Thermo Fisher) and a UV-Vis detector set to 361 nm as described [48]. Corrinoids were separated on a Hypersil Gold C18 column (Thermo Fisher, 1.9 μm pore size, 2.1 mm inner diameter × 50 mm length) at a flow rate of 0.2 mL min^{-1} at 30 °C using 2.5 mM ammonium acetate in water as eluent A and 100% methanol as eluent B. The mobile phase was 100% eluent A and 0% eluent B for 0.46 min, followed by linear increases to 15% eluent B after 0.81 min, 50% eluent B after 3.32 min, and 90% eluent B after 5.56 min and a 0.3-min hold before equilibration to initial column conditions. Corrinoid mass spectra were collected in positive ionization mode using a HESI II electrospray ionization source (Thermo Fisher) with a *m/z* scan ranging from 1,000–1,500 and a resolution of 140,000. The detection limit for this LC-MS method was 2.5 ng of corrinoid.

NMR spectroscopy

Growth of *Dsf hafniense* strain Y51 in twelve 2.2-L vessels yielded approximately 22 liters of cell culture suspension. Each vessel received neat TCE (400 μL, 2.3 mM aqueous concentration), yeast extract (2 g/L) and Cbi (0.5 μM) to enhance corrinoid production. Cells were harvested after three TCE amendments (a total of 1,200 μL) were completely dechlorinated to *c*DCE. Total intracellular corrinoids were extracted and the predominant corrinoid-containing fraction was obtained following HPLC separation and manual collection from the detector outlet informed by the detector response at 361 nm. Approximately 0.7 mg of purified corrinoid was dissolved in methanol-*d4* (250 μL) to conduct ^{1}H and COSY NMR experiments using an INOVA 600 MHz NMR spectroscopy system (Varian). The ^{1}H NMR experiments consisted of 1,024 scans, using PRESAT solvent suppression multiple peak selection, and a total measuring time of 1 hour. The gradient-selected COSY NMR experiments consisted of 256 scans per increment at 96 increments. The delay time between scans was 1.5 sec, and the total measuring time was 1 hour.

Blue native polyacrylamide gel electrophoresis (BN-PAGE), enzyme assays and proteomic analysis

Dsf hafniense strain JH1 cells were harvested from 100 mL cultures and the crude protein extracts were prepared as described [49]. BN-PAGE using pre-cast 4 to 16% gradient Bis-Tris gel (Thermo Fisher) stained with Coomassie Blue was performed following the NativePAGE™ Bis-Tris Gel Protocol [49]. Gel lanes were loaded with 25 μL of protein standards or crude protein extracts containing approximately 6 μg of total protein as estimated with the Bradford assay [50]. Electrophoresis used chilled buffers and a BN-PAGE chamber placed in an ice bath, and separation occurred for 60 min at 150 V and then for another 45 min at 200 V. The blank, ladder and sample lanes were separated and stained according to the fast Coomassie G-250 staining protocol (Thermo Fisher). The gel slices

were cut based on molecular mass ranges as visualized by the protein standards in the ladder lane. Enzyme assays to detect dechlorinating activity were conducted with *Dsf hafniense* strain JH1 cell lysate (positive control) and individual gel slices inside an anoxic chamber (Coy Laboratory) as described [49]. The assays (1 mL) were conducted in 2-mL sealed glass vials containing 100 mM Tris-HCl buffer (pH 7.4) amended with 2 mM titanium citrate, 2 mM methyl viologen, and 2 mM TCE. Each assay mixture was incubated in an anoxic chamber for 24 h and analyzed for *c*DCE formation using gas chromatography [49]. In-gel digestion and MS analysis were performed at the BioZone Mass Spectrometry Facility (University of Toronto, Toronto, Canada) using X! Tandem for peptide/protein identification (The GPM, thegpm.org; version X! Tandem Vengeance (2015.12.15.2)) [49]. X! Tandem was set up to search for tryptic peptides based on the *Dsf hafniense* strain Y51 genome, all characterized RDases, other *Dsf* proteins in the NCBI database, as well as common contaminants such as human keratins and trypsin (total of 33,950 proteins) using a fragment ion mass tolerance of 0.40 Da and a parent ion tolerance of 2.5 Da. Deamidation of asparagine and glutamine, oxidation of methionine and tryptophan, N-terminal ammonia loss, or cyclization of glutamine or glutamamic acid to pyroglutamine or pyroglutamic acid were allowed in X! Tandem as possible peptide modifications. Further validation and refinement was performed using Scaffold software version 4.5.3 (Proteome Software Inc.) with a reverse decoy database to establish a false discovery rate. Peptide identifications were accepted as valid at a Peptide Prophet probability of greater than 95% [51]. Subsequent protein identifications were considered valid at a Protein Prophet probability of greater than 99% [52], which were filtered to include those that had at least two unique peptide identifications.

Primer and probe design

Primers and TaqMan probe targeting the *pceA* gene in *Dsf hafniense* strain Y51 (locus # DSY2839), *Dhb restrictus* strain PER-K23 (locus # DEHRE_12145), and *pceA* homologs (>95% sequence identity) identified in other *Dsf* and *Dhb* strains (GenBank accession numbers CAD28792.1, CDX02974.1, AAO60101.1 and AIA58680.1) were designed using Primer Express software (Applied Biosystems). A consensus region of the *Dsf* and *Dhb pceA* gene sequences was selected to meet the quantitative PCR (qPCR) design criteria of (i) an amplicon size between 50–150 bp, (ii) a primer melting temperature (T_m) of 58–60 °C, and (iii) a probe T_m of 68–70 °C [53]. The G+C content of the primers and probe was between 30 to 80 mol %, with no more than three consecutive G or C bases in either the primer or the probe sequences. The specificity of the forward primer Df_pceA_1223F (5′-CGGACAAGCCGAGAAAATTC-3′), the reverse primer Df_pceA_1286R (5′-GCATCCGCACATTTTTTGC-3′) and the probe Df_pceA_1247probe (5′-6FAM-TACGCGAGTTCTGCCG-MGB-3′) to *pceA* genes was verified by using BLAST search against the NCBI database.

Chemical and molecular analyses

Ethene and chlorinated compounds were quantified in triplicate cultures using an Agilent 7890 gas chromatograph as described [10]. The two-step dechlorination processes PCE-to-*c*DCE (*Dhb)* and *c*DCE-to-ethene (*Dhc*) were measured based on the quantification of daughter and end products, TCE/*c*DCE and VC/ethene, respectively. Each dechlorination step is associated with the release of one chloride ion and the PCE-to-*c*DCE and *c*DCE-to-

ethene dechlorination rates were reported as μM Cl^- released per day. The list of potential molecular formulas for the lower base of the *Dsf* cobamide was generated using the web-based platform ChemCalc [54]. To obtain genomic DNA, cells from 1 mL culture suspension were harvested via vacuum filtration onto a 0.22 μm polyvinylidene difluoride membrane filter (Merck Millipore Ltd.) and processed using the MO BIO Soil DNA Isolation kit (MO BIO) as described [45]. *Dhc* 16S rRNA gene-targeted qPCR was performed following established protocols using primer set Dhc1200F/Dhc1271R and TaqMan probe Dhc1240probe [53]. The qPCR assay targeting the *Dhb pceA* gene with the newly designed primers and probe used identical qPCR conditions. Standard curves were generated using a serial dilution of plasmid pMK-RQ (Life Technologies) with a *Dsf hafniense* strain Y51 *pceA* fragment (1,656 bp) insertion. The *pceA* qPCR assay standard curve had a slope of −3.785, a y-intercept of 40.41, a R^2 of 0.999, and a PCR amplification efficiency of 83.8%. The assay spanned a linear range from 4.64×10^1 to 4.64×10^8 *pceA* gene copies per reaction, with 4.6 *pceA* gene copies per reaction as the detection limit. All qPCR assays used template DNA samples extracted from triplicate cultures, and standard curves were generated from three independently prepared serial dilutions of the respective plasmid DNA standards.

Statistical analysis

The PCE-to-*c*DCE dechlorination rates from three independent *Dhb* cultures grown with purinyl-Cba or vitamin B_{12} were statistically compared. The two-sample *t*-test was carried out using the data analysis tool provided in Microsoft Excel 2016.

Bioinformatics and phylogenetic analyses

RDase sequence alignments and identity comparisons were performed with Clustal Omega (www.ebi.ac.uk/Tools/msa/clustalo) [55]. Reciprocal BLAST analysis was used to query the sequenced *Dsf* genomes and search for orthologous *bza* genes implicated in anaerobic DMB biosynthesis [47]. Twenty CobT amino acid sequences from the genomes of nine *Dsf* strains, five *Dhb* strains and six *Desulfosporosinus* strains, along with 20 CobT and homologous protein (i.e., ArsA and ArsB) sequences from other bacteria (Supplementary Table 2) were retrieved from GenBank, and aligned using the MUSCLE plug-in in Geneious 8.1.7 with 10 iterations. The phylogenetic tree of CobT and homologous proteins was constructed using the PHMYL maximum likelihood tree builder plug-in in Geneious 8.1.7 with 100 bootstraps and the Le Gascuel substitution model [56].

Heterologous expression and purification of CobT

The pET-28a(+) vector (EMD Millipore) was used to clone and express *cobT* carrying an N-terminal hexa-histidine tag. *Dsf cobT* (locus # DSY2114) and *Dhc cobT* (locus # DehaBAV1_0626) were amplified using Phusion Flash High-Fidelity PCR Master Mix (Thermo Fisher) and primer sets NJ459-NJ460 and NJ461-NJ462 (Supplementary Table 4), respectively, using genomic DNA from *Dsf* strain Y51 and *Dhc* strain BAV1 axenic cultures. PCR products were cleaned using the UltraClean® PCR Clean-Up Kit (MO BIO). The pET-28a(+) vector backbone was digested with EcoRI and NdeI, dephosphorylated with rSAP, and gel extracted to remove remaining supercoiled constructs. The prepared plasmids pNJ050 and pNJ049 (Supplementary Table 5), which contain *Dsf cobT* and *Dhc cobT*

inserts, respectively, were then transformed into BW25113 electrocompetent cells with pre-induced λ Red recombinase from plasmid pKD46 for homologous recombination [57]. Following sequence verification, recombinant vectors were introduced into *E. coli* strain BL21(DE3) (New England Biolabs) for overexpression and purification.

Enzyme expression and purification were performed as described with modifications [58]. In brief, *E. coli* strain BL21(DE3) carrying a *cobT* expression plasmid was grown in 1 L of Terrific Broth (Thermo Fisher) with 50 μg/mL kanamycin at 37 °C and 180 rpm to an OD_{600} of 0.8. Cultures were induced with 0.4 mM isopropyl β-D-1-thiogalactopyranoside (Thermo Fisher) and incubated overnight at 16 °C and 180 rpm. Cells were collected by centrifugation at 9,000 × g for 20 min, suspended in HEPES buffer (50 mM HEPES, 300 mM NaCl and 10 mM imidazole, pH 7.5), and sonicated in an ice bath for 45 min (3-sec on and 4-sec off). The lysate was centrifuged at 38,000 × g for 20 min and the supernatant was passed through a 25-mL glass column containing about 0.5 mL Ni-NTA resin (Qiagen). After washing with HEPES buffer (20 mM imidazole), proteins were eluted with 5–7 mL of HEPES buffer containing 250 mM imidazole and 5 % (w/v) glycerol. Protein concentrations were estimated using the Bradford assay [50] and protein purity was examined by SDS-PAGE and Coomassie Blue staining. The protein stock solutions (*Dsf* Y51 CobT, 15 mg/mL; *Dhc* BAV1 CobT, 10 mg/mL) were frozen in liquid nitrogen and stored at –80 °C. The N-terminal hexa-histidine tag was retained for all experiments.

In vitro CobT activity

CobT assays were performed as described [59]. Briefly, each reaction (300 μL) contained 30 μg CobT (corresponding to a final enzyme concentration of ~2.6 μM), 2 mM NaMN, 10 mM $MgCl_2$, and 0.25 mM of either purine or DMB in 50 mM pH 7.5 Tris-HCl buffer. The assay vials were incubated at 30 °C for 30 min before the reactions were terminated by the addition of 15 μL formic acid (≥88%, w/v) and then transferred to a boiling water bath for 1 min. Following neutralizing the pH with 5 M NaOH, precipitated protein was removed by centrifugation at 13,000 × g for 5 min. Lower bases and their respective α-RPs were analyzed by injecting 10 μL samples into an Agilent Technologies 1200 series HPLC system equipped with a diode array detector set to 262 nm. Separation was performed with an Eclipse XDB-C18 column (5 μm pore size, 4.6 mm inner diameter × 250 mm length) at a flow rate of 1 mL per min at 30 °C using 0.1% (v/v) formic acid in water as eluent A and 0.1% (v/v) formic acid in methanol as eluent B. The initial mobile phase and time parameters for the gradient elution were as follows: t = 0, 15% eluent B, 85% eluent A; t = 5 min, 25% eluent B, 75% eluent A; t = 11 min, 85% eluent B, 15% eluent A, t = 15 min, end of run. To obtain material for subsequent MS analysis, semi-preparative HPLC was performed using the method outlined above with minor modification as follows. The injection volume was increased to 100 μL, and a 1-mL fraction containing α-RP [DMB] or α-RP [Purine] was manually collected from the detector outlet once the target peak was detected. Three such injections were performed and the α-RP fractions from each were combined, and then concentrated 10-fold from 3 mL to 300 μL using a Savant ISS110 vacuum dryer (Thermo Fisher). Aliquots (10 μL) of the concentrated α-RP solutions were introduced into an Exactive Plus Orbitrap MS via direct injection. The analytes were ionized

using electrospray ionization operated in positive mode and detected via high-resolution MS with a mass range of 200 to 400 *m/z* [10].

Data availability

All data generated or analyzed in this study are included in this published article and its supplementary information files.

Supplementary Material

Refer to Web version on PubMed Central for supplementary material.

Acknowledgments

We thank Dr. Julien Maillard, École Polytechnique Fédérale de Lausanne, France, for providing *Dhb restrictus* strain PER-K23. This research was supported by a grant from the Superfund Research Program under the National Institute of Environmental Health Sciences (R01ES024294) to F.E.L., with additional support provided by the Strategic Environmental Research and Development Program (SERDP project ER-2312) to F.E.L. Y. Yin acknowledges the financial support from the China-UT One-Hundred Scholars Program by the China Scholarship Council and the University of Tennessee.

References

1. Renz P. Chemistry and biochemistry of B_{12}. Banerjee R, editorJohn Wiley & Sons, Inc; 1999. 558–572.
2. Gruber K, Puffer B, Kräutler B. Vitamin B_{12}-derivatives—enzyme cofactors and ligands of proteins and nucleic acids. Chem Soc Rev. 2011; 40:4346–4363. [PubMed: 21687905]
3. Kräutler B, et al. The cofactor of tetrachloroethene reductive dehalogenase of *Dehalospirillum multivorans* is norpseudo-B_{12}, a new type of a natural corrinoid. Helv Chim Acta. 2003; 86:3698–3716.
4. Im J, Walshe-Langford GE, Moon JW, Löffler FE. Environmental fate of the next generation refrigerant 2,3,3,3-tetrafluoropropene (HFO-1234yf). Environ Sci Technol. 2014; 48:13181–13187. [PubMed: 25329364]
5. Maillard J, et al. Characterization of the corrinoid iron-sulfur protein tetrachloroethene reductive dehalogenase of *Dehalobacter restrictus*. Appl Environ Microbiol. 2003; 69:4628–4638. [PubMed: 12902251]
6. Liao RZ, Chen SL, Siegbahn PEM. Which oxidation state initiates dehalogenation in the B_{12}-dependent enzyme NpRdhA: Co^{II}, Co^{I}, or Co^{0}? ACS Catalysis. 2015; 5:7350–7358.
7. Bommer M, et al. Structural basis for organohalide respiration. Science. 2014; 346:455–458. [PubMed: 25278505]
8. Payne KAP, et al. Reductive dehalogenase structure suggests a mechanism for B_{12}-dependent dehalogenation. Nature. 2015; 517:513–516. [PubMed: 25327251]
9. Löffler FE, et al. *Dehalococcoides mccartyi* gen nov., sp nov., obligately organohalide-respiring anaerobic bacteria relevant to halogen cycling and bioremediation, belong to a novel bacterial class, *Dehalococcoidia* classis nov., order *Dehalococcoidales* ord nov and family *Dehalococcoidaceae* fam nov., within the phylum *Chloroflexi*. Int J Syst Evol Microbiol. 2013; 63:625–635. [PubMed: 22544797]
10. Yan J, et al. The corrinoid cofactor of reductive dehalogenases affects dechlorination rates and extents in organohalide-respiring *Dehalococcoides mccartyi*. ISME J. 2016; 10:1092–1101. [PubMed: 26555247]
11. Yi S, et al. Versatility in corrinoid salvaging and remodeling pathways supports corrinoid-dependent metabolism in *Dehalococcoides mccartyi*. Appl Environ Microbiol. 2012; 78:7745–7752. [PubMed: 22923412]

12. Mok KC, Taga ME. Growth inhibition of *Sporomusa ovata* by incorporation of benzimidazole bases into cobamides. J Bacteriol. 2013; 195:1902–1911. [PubMed: 23417488]
13. Stupperich E, Eisinger HJ, Kräutler B. Identification of phenolyl cobamide from the homoacetogenic bacterium *Sporomusa ovata*. Eur J Biochem. 1989; 186:657–661. [PubMed: 2606109]
14. Villemur R, Lanthier M, Beaudet R, Lepine F. The *Desulfitobacterium* genus. FEMS Microbiol Rev. 2006; 30:706–733. [PubMed: 16911041]
15. Ding C, Zhao S, He J. A *Desulfitobacterium* sp strain PR reductively dechlorinates both 1,1,1-trichloroethane and chloroform. Environ Microbiol. 2014; 16:3387–3397. [PubMed: 24428759]
16. Suyama A, Yamashita M, Yoshino S, Furukawa K. Molecular characterization of the PceA reductive dehalogenase of *Desulfitobacterium* sp strain Y51. J Bacteriol. 2002; 184:3419–3425. [PubMed: 12057934]
17. Reinhold A, et al. Impact of vitamin B_{12} on formation of the tetrachloroethene reductive dehalogenase in *Desulfitobacterium hafniense* strain Y51. Appl Environ Microbiol. 2012; 78:8025–8032. [PubMed: 22961902]
18. Nonaka H, et al. Complete genome sequence of the dehalorespiring bacterium *Desulfitobacterium hafniense* Y51 and comparison with *Dehalococcoides ethenogenes* 195. J Bacteriol. 2006; 188:2262–2274. [PubMed: 16513756]
19. Crofts TS, Seth EC, Hazra AB, Taga ME. Cobamide structure depends on both lower ligand availability and CobT substrate specificity. Chem Biol. 2013; 20:1265–1274. [PubMed: 24055007]
20. Yan J, Im J, Yang Y, Löffler FE. Guided cobalamin biosynthesis supports *Dehalococcoides mccartyi* reductive dechlorination activity. Phil Trans R Soc B. 2013; 368:20120320. [PubMed: 23479750]
21. Keller S, et al. Exogenous 5,6-dimethylbenzimidazole caused production of a non-functional tetrachloroethene reductive dehalogenase in *Sulfurospirillum multivorans*. Environ Microbiol. 2013; 16:3361–3369. [PubMed: 24433392]
22. Guimarães DH, Weber A, Klaiber I, Vogler B, Renz P. Guanylcobamide and hypoxanthylcobamide-corrinoids formed by *Desulfovibrio vulgaris*. Arch Microbiol. 1994; 162:272–276.
23. Stasyuk OA, Szatyłowicz H, Krygowski TM. Effect of the H-bonding on aromaticity of purine tautomers. J Org Chem. 2012; 77:4035–4045. [PubMed: 22448684]
24. Moffatt BA, Ashihara H. Purine and pyrimidine nucleotide synthesis and metabolism. The Arabidopsis Book. 2002; 1:e0018–20. 1–20. [PubMed: 22303196]
25. Kublik A, et al. Identification of a multi-protein reductive dehalogenase complex in *Dehalococcoides mccartyi* strain CBDB1 suggests a protein-dependent respiratory electron transport chain obviating quinone involvement. Environ Microbiol. 2016; 18:3044–3056. [PubMed: 26718631]
26. Dobbek H, Svetlitchnyi V, Gremer L, Huber R, Meyer O. Crystal structure of a carbon monoxide dehydrogenase reveals a [Ni-4Fe-5S] cluster. Science. 2001; 293:1281–1285. [PubMed: 11509720]
27. Iverson TM, Luna-Chavez C, Cecchini G, Rees DC. Structure of the *Escherichia coli* fumarate reductase respiratory complex. Science. 1999; 284:1961–1966. [PubMed: 10373108]
28. Rosemeyer H. The chemodiversity of purine as a constituent of natural products. Chem Biodivers. 2004; 1:361–401. [PubMed: 17191854]
29. Löfgren N, Lüning B. On the structure of nebularine. Acta Chem Scand. 1953; 7:225–225.
30. Nakamura G. Studies on antibiotic actinomycetesIII on *Streptomyces* producing 9-β-D-ribofuranosylpurine. J Antibiot. 1961; 14:94–97.
31. Cooper R, Horan AC, Gunnarsson I, Patel M, Truumees I. Nebularine from a novel *Microbispora* sp. J Ind Microbiol. 1986; 1:275–276.
32. Gordon MP, Brown GB. A study of the metabolism of purine riboside. J Biol Chem. 1956; 220:927–937. [PubMed: 13331950]
33. Brown EG, Konuk M. Plant cytotoxicity of nebularine (purine riboside). Phytochemistry. 1994; 37:1589–1592.

34. el Kouni MH, Messier NJ, Cha S. Treatment of schistosomiasis by purine nucleoside analogues in combination with nucleoside transport inhibitors. Biochem Pharmacol. 1987; 36:3815–3821. [PubMed: 3689423]
35. Brown EG, Konuk M. Biosynthesis of nebularine (purine 9-β-d-ribofuranoside) involves enzymic release of hydroxylamine from adenosine. Phytochemistry. 1995; 38:61–71.
36. Ralevic V, Burnstock G. Receptors for purines and pyrimidines. Pharmacol Rev. 1998; 50:413–492. [PubMed: 9755289]
37. Burnstock G. Purinergic signalling and disorders of the central nervous system. Nat Rev Drug Discov. 2008; 7:575–590. [PubMed: 18591979]
38. Virgilio FD, Adinolfi E. Extracellular purines, purinergic receptors and tumor growth. Oncogene. 2017; 36:293–303. [PubMed: 27321181]
39. Miles ZD, McCarty RM, Molnar G, Bandarian V. Discovery of epoxyqueuosine (oQ) reductase reveals parallels between halorespiration and tRNA modification. Proc Natl Acad Sci USA. 2011; 108:7368–7372. [PubMed: 21502530]
40. Parks JM, et al. The genetic basis for bacterial mercury methylation. Science. 2013; 339:1332–1335. [PubMed: 23393089]
41. Randaccio L, Geremia S, Demitri N, Wuerges J. Vitamin B_{12}: unique metalorganic compounds and the most complex vitamins. Molecules. 2010; 15:3228–3259. [PubMed: 20657474]
42. Schneider Z. Comprehensive B_{12}: Chemistry, Biochemistry, Nutrition, Ecology, Medicine. Schneider Z, Stroiński A, editorsWalter de Gruyter & Co; 1987. 93–104.
43. Degnan PH, Taga ME, Goodman AL. Vitamin B_{12} as a modulator of gut microbial ecology. Cell Metab. 2014; 20:769–778. [PubMed: 25440056]
44. Suyama A, et al. Isolation and characterization of *Desulfitobacterium* sp strain Y51 capable of efficient dehalogenation of tetrachloroethene and polychloroethanes. Biosci Biotechnol Biochem. 2001; 65:1474–1481. [PubMed: 11515528]
45. Yan J, Ritalahti KM, Wagner DD, Löffler FE. Unexpected specificity of interspecies cobamide transfer from *Geobacter* spp. to organohalide-respiring *Dehalococcoides mccartyi* strains. Appl Environ Microbiol. 2012; 78:6630–6636. [PubMed: 22773645]
46. Holliger C, et al. *Dehalobacter restrictus* gen. nov and sp nov., a strictly anaerobic bacterium that reductively dechlorinates tetra- and trichloroethene in an anaerobic respiration. Arch Microbiol. 1998; 169:313–321. [PubMed: 9531632]
47. Hazra AB, et al. Anaerobic biosynthesis of the lower ligand of vitamin B_{12}. Proc Natl Acad Sci USA. 2015; 112:10792–10797. [PubMed: 26246619]
48. Wang PH, et al. Refined experimental annotation reveals conserved corrinoid autotrophy in chloroform-respiring *Dehalobacter* isolates. ISME J. 2017; 11:626–640. [PubMed: 27898054]
49. Tang S, et al. Functional characterization of reductive dehalogenases by using blue native polyacrylamide gel electrophoresis. Appl Environ Microbiol. 2013; 79:974–981. [PubMed: 23204411]
50. Bradford MM. A rapid and sensitive method for the quantification of microgram quantities of protein utilizing the principle of protein-dye binding. Anal Biochem. 1976; 72:248–254. [PubMed: 942051]
51. Keller A, Nesvizhskii AI, Kolker E, Aebersold R. Empirical statistical model to estimate the accuracy of peptide identifications made by MS/MS and database search. Anal Chem. 2002; 74:5383–5392. [PubMed: 12403597]
52. Nesvizhskii AI, Keller A, Kolker E, Aebersold R. A statistical model for identifying proteins by tandem mass spectrometry. Anal Chem. 2003; 75:4646–4658. [PubMed: 14632076]
53. Ritalahti KM, et al. Quantitative PCR targeting 16S rRNA and reductive dehalogenase genes simultaneously monitors multiple *Dehalococcoides* strains. Appl Environ Microbiol. 2006; 72:2765–2774. [PubMed: 16597981]
54. Patiny L, Borel A. ChemCalc: A building block for tomorrow's chemical infrastructure. J Chem Inf Model. 2013; 53:1223–1228. [PubMed: 23480664]
55. Sievers F, et al. Fast, scalable generation of high-quality protein multiple sequence alignments using Clustal Omega. Mol Syst Biol. 2011; 7:539. [PubMed: 21988835]

56. Kearse M, et al. Geneious Basic: an intergrated and extendable desktop software platform for the organization and analysis of sequence data. Bioinformatics. 2012; 28:1647–1649. [PubMed: 22543367]

57. Datsenko KA, Wanner BL. One-step inactivation of chromosomal genes in *Escherichia coli* K-12 using PCR products. Proc Natl Acad Sci USA. 2000; 97:6640–6645. [PubMed: 10829079]

58. Huang L, et al. A family of metal-dependent phosphatases implicated in metabolite damage-control. Nat Chem Biol. 2016; 12:621–627. [PubMed: 27322068]

59. Hazra AB, Tran JLA, Crofts TS, Taga ME. Analysis of substrate specificity in CobT homologs reveals widespread preference for DMB, the lower axial ligand of vitamin B_{12}. Chem Biol. 2013; 20:1275–1285. [PubMed: 24055005]

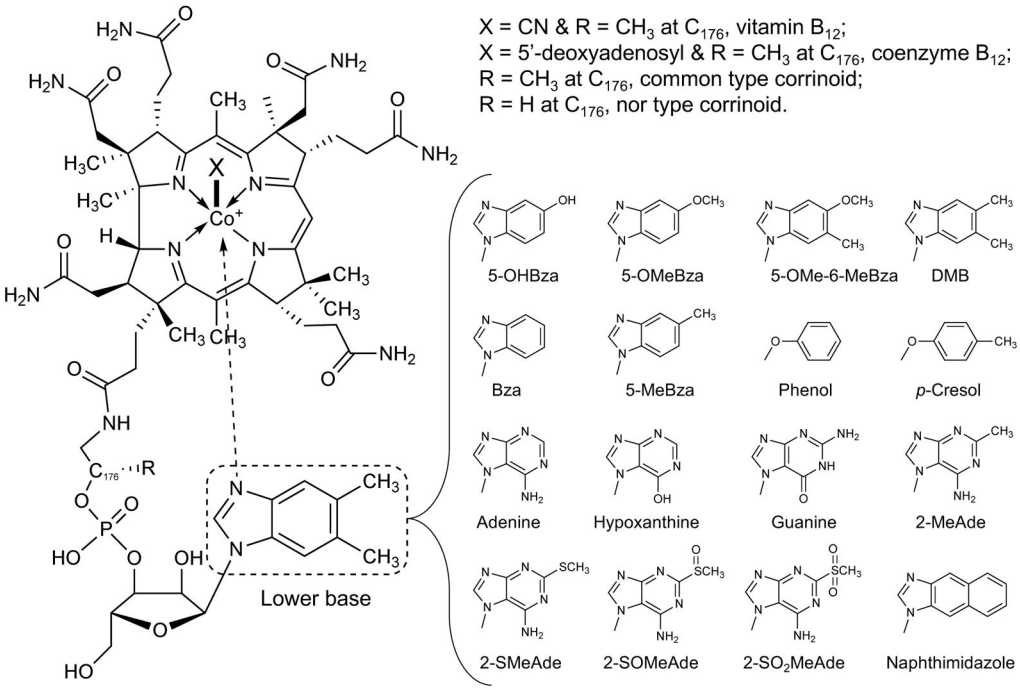

Figure 1. Cobamide general structure and the 16 known lower bases found in naturally occurring cobamides

Variations in cobamide structures are found in the Coβ upper ligand, the side chain at position C_{176}, and the Coα lower base. Abbreviations: 5-OHBza, 5-hydroxybenzimidazole; 5-OMeBza, 5-methoxybenzimidazole; 5-OMe-6-MeBza, 5-methoxy-6-methylbenzimidazole; DMB, 5,6-dimethylbenzimidazole; Bza, benzimidazole; 5-MeBza, 5-methylbenzimidazole; 2-MeAde, 2-methyladenine; 2-SMeAde, 2-methylmercaptoadenine; 2-SOMeAde, 2-methylsulfinyladenine; 2-SO_2MeAde, 2-methylsulfonyladenine.

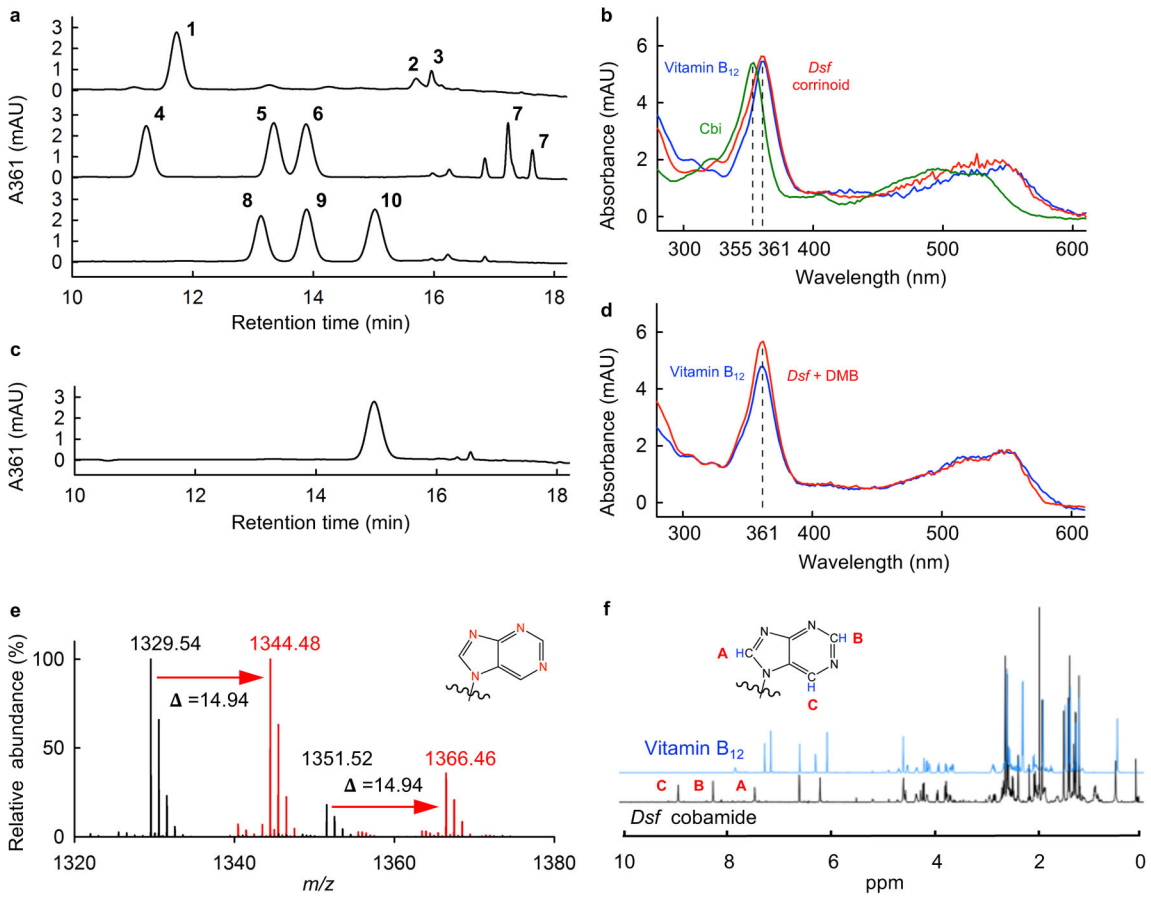

Figure 2. Spectrophotometric and structural features of *Desulfitobacterium* native corrinoids

(**a**) HPLC chromatograms of the native corrinoids produced by *Dsf hafniense* strain Y51 eluted at 11.79 min (**1**), 15.74 min (**2**) and 15.94 min (**3**). The predominant corrinoid peak at 11.79 min accounted for 86% of the total corrinoids produced by strain Y51 based on 361 nm peak area integration. Cobamide standards (5 mg/L each) were norpseudo vitamin B_{12} (**4**), 11.23 min; Bza-Cba (**5**), 13.34 min; 5-OMeBza-Cba (**6**), 13.88 min; *p*-Cresol-Cba (**7**), 17.23 min and 17.64 min; 5-OHBza-Cba (**8**), 13.13 min; 5-MeBza-Cba (**9**), 13.89 min; vitamin B_{12} (**10**), 15.02 min. (**b**) UV-Vis spectra (250–600 nm) of cobinamide, vitamin B_{12} and the 11.79 min native *Dsf* corrinoid. (**c**) HPLC chromatogram and (**d**) UV-Vis spectrum of the non-native cobamide produced in strain Y51 cultures with 25 μM DMB amendment. (**e**) Mass spectra of ^{15}N-labeled and unlabeled native *Dsf* corrinoid. Mass shifts in $[M+H]^+$ and $[M+Na]^+$ values confirmed that the *Dsf* cobamide contains four N atoms in the lower base structure. (**f**) The superimposed ^{1}H NMR spectra of the *Dsf* corrinoid (black line) and the vitamin B_{12} standard (blue line).

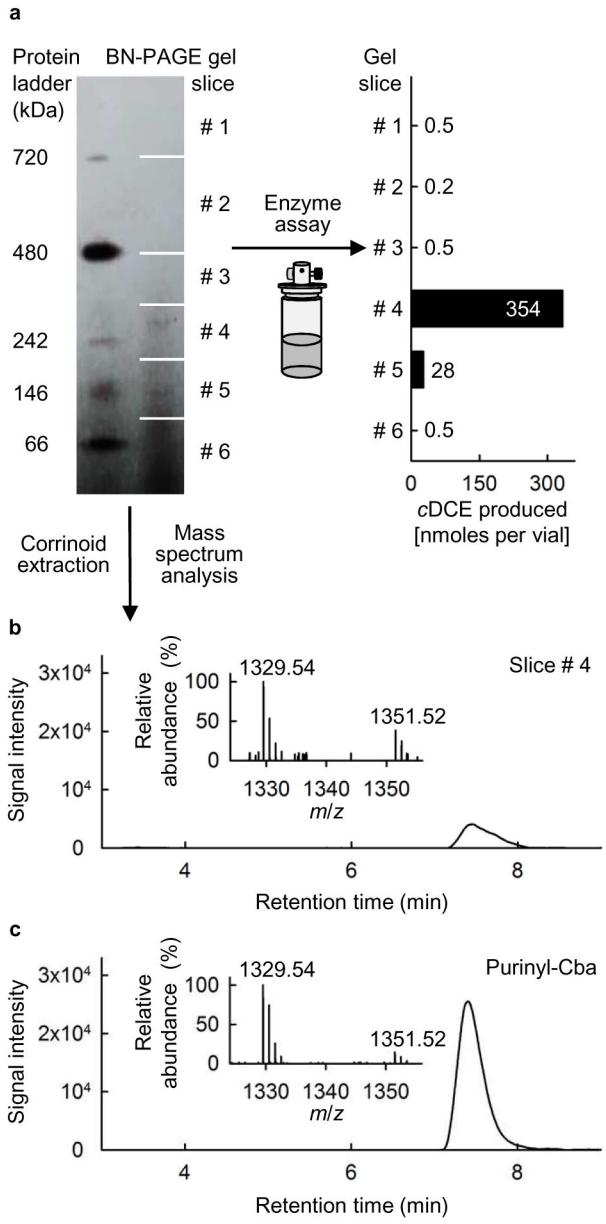

Figure 3. Identification of purinyl-Cba as the native prosthetic group in *Dsf* PCE RDase following non-denaturing, gel-electrophoretic separation of *Dsf* crude protein extracts using BN-PAGE

(**a**) TCE-to-*c*DCE dechlorination activity of different BN-PAGE gel slices measured using dehalogenation enzyme assays. (**b**,**c**) UPLC separation and mass spectrometry analysis of the corrinoid recovered from BN-PAGE gel slice #4 showing the highest dechlorination activity (**b**) and the purinyl-Cba standard (0.25 mg/L) (**c**).

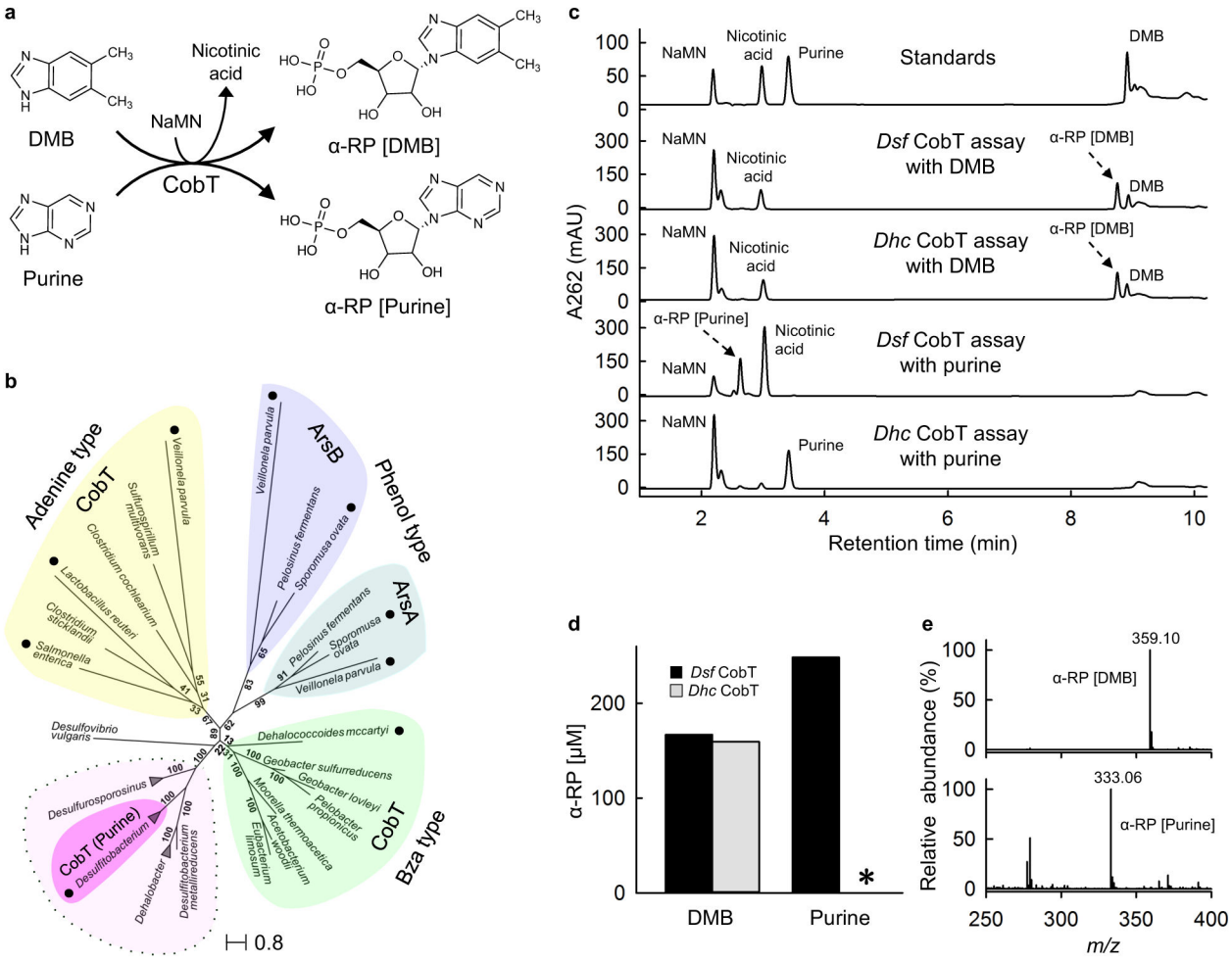

Figure 4. Phylogenetic analysis of CobT homologous proteins and substrate specificity of *Dsf* CobT

(**a**) The *Dsf* CobT activated DMB or purine to their respective alpha-ribazole-5′-phosphate (α-RP) forms. (**b**) Phylogenetic relationship of 40 CobT and homologous proteins from phylogenetically diverse corrinoid-auxotrophic and prototrophic bacteria. Solid black dots indicate CobT enzymes with biochemically determined substrate specificities. CobT enzymes of other members of the Peptococcaceae may share catalytic features with the *Dsf* CobT and activate purine as a lower base for cobamide biosynthesis (indicated by the dashed line-enclosed pink area). (**c**) HPLC analysis demonstrating purified CobT activity with NaMN and a lower base as the substrates. The small peak to the left of nicotinic acid in the bottom trace (*Dhc* CobT assay with purine) has a similar retention time as α-RP [purine] shown in the panel above, but spectral analysis revealed distinct absorbance features. (**d**) The formation of α-RP [DMB] or α-RP [purine] in CobT assays with DMB or purine provided as a lower base substrate. The α-RP concentrations were calculated based on the concentration decreases of the respective lower base substrates. Data are averages of measurements from duplicate assays. The (*) indicates that no α-RP [purine] production was observed in *Dhc* CobT assays with purine as the lower base. (**e**) Mass spectrometry analysis of α-RP [DMB] and α-RP [purine] formed in CobT enzyme assays.

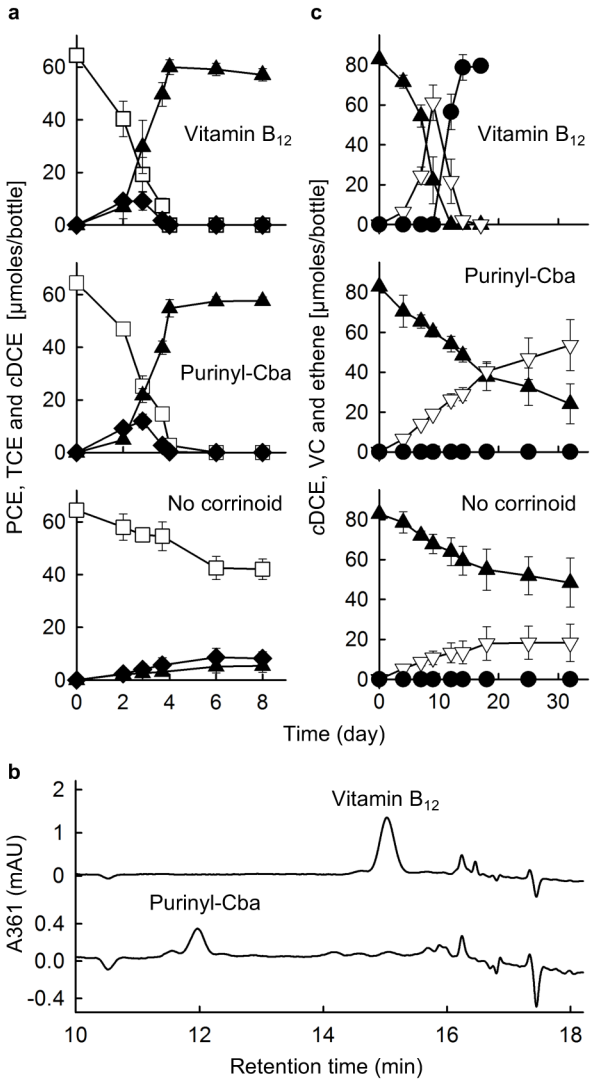

Figure 5. Effects of purinyl-Cba substitution for vitamin B_{12} on the activity of corrinoid-auxotrophic, organohalide-respiring bacteria

(**a**) Reductive dechlorination activity in *Dhb restrictus* cultures supplied with PCE as electron acceptor and 36.9 nM vitamin B_{12} (positive control), 36.9 nM purinyl-Cba, or no corrinoid addition (negative control). (**b**) HPLC chromatograms of the total intracellular corrinoids extracted from vitamin B_{12}- or purinyl-Cba-amended *Dhb* cultures. Purinyl-Cba was the only cobamide recovered from purinyl-Cba-amended *Dhb* cultures. (**c**) Reductive dehalogenation of *c*DCE to ethene in *Dhc* strain BAV1 cultures amended with 36.9 nM vitamin B_{12} (positive control), 36.9 nM purinyl-Cba, or no corrinoid addition (negative control). Squares, PCE; solid diamonds, TCE; solid triangles, *c*DCE; inverted triangles, vinyl chloride; solid circles, ethene. Error bars represent mean values ± standard deviation from three independent cultures.